Journal of the European Ceramic Society 22 (2002) 2749–2756

www.elsevier.com/locate/jeurceramsoc

High-temperature active/passive oxidation and bubble formation of CVD SiC in O_2 and CO_2 atmospheres

Takashi Goto*, Hisashi Homma

Institute for Materials Research, Tohoku University 2-1-1 Katahira, Aoba-ku, Sendai 980-8577, Japan

Received 12 October 2001; received in revised form 20 January 2002; accepted 20 February 2002

Abstract

The active oxidation, passive oxidation and bubble formation of CVD SiC were studied in O_2 and CO_2 at temperatures from 1650 to 2000 K. The active oxidation rates in O_2 increased with increasing oxygen partial pressure (P_{O_2}); however, those in CO_2 showed the maxima at specific P_{O_2}. The passive oxidation kinetics in O_2 were either linear–parabolic or parabolic depending on temperature and P_{O_2}, whereas that in CO_2 was always parabolic. The activation energies for the parabolic oxidation in O_2 and CO_2 were 210 and 150 kJ/mol, respectively, suggesting different rate-determining process in these atmospheres. The bubble formation was controlled by temperature and P_{O_2} being independent of oxidant gas species. The linear and parabolic oxidation rates were accelerated by the bubble formation.

Keywords: Chemical vapor deposition; Corrosion; SiC; Structural applications; Surfaces

1. Introduction

Silicon-based ceramics such as silicon carbide (SiC) and silicon nitride (Si_3N_4) are widely studied because of their potential as high temperature structural materials, due to excellent high-temperature mechanical properties and oxidation resistance.[1] The oxidation behavior of SiC has been investigated using mainly sintered bodies. Since the oxidation of SiC is strongly affected by impurity or additives, highly pure and dense specimens such as CVD SiC should be used to understand the intrinsic oxidation behavior.[2] On the other hand, CVD SiC is also used for coatings such as a nose cone of space vehicle and combustion chambers. Therefore, it is practically important to study the oxidation of CVD SiC in wide-ranged oxygen partial pressures at high temperatures.

The oxidation behavior of SiC can be classified into three features, i.e. active oxidation, passive oxidation and bubble formation. Many reports have been published on the passive oxidation of SiC mainly in O_2.[2] A few papers report the oxidation of SiC in CO_2;[3–5] however, the oxidation kinetics have not been investigated in detail. The bubble formation is an important issue to use SiC at extremely high temperatures. Although several papers have dealt with this phenomenon briefly,[6,7] no research on the bubble formation has been conducted in CO_2 atmosphere.

In this paper, these three distinct oxidation behaviors have been studied by using CVD SiC in CO_2 and O_2 atmospheres at high temperatures from 1650 to 2000 K.

2. Experimental

Yellow-colored translucent CVD SiC plates (0.6 mm in thick, β-type, Admap, Japan) were used as specimens. The impurity level is ppb according to the analysis of manufactures, and (111) plane is strongly oriented to the surface. The specimens were cut to a disk with 10 mm in diameter, and were mirror-polished. An electric furnace with cubic zirconia heaters was used to increase the temperature up to 2473 K. The mass changes were continuously monitored by an electro-balance (Cahn, D-101, USA, sensitivity 1 μg). A zirconia wire with a hook was used to hold the specimen in the furnace. The specimens were heated in a flowing Ar gas. At a specific temperature, oxidant gases (i.e. O_2–Ar, CO–CO_2 and

* Corresponding author. Tel.: +81-22-215-2105; fax: +81-22-215-2107.

E-mail address: goto@imr.edu (T. Goto).

0955-2219/02/$ - see front matter
PII: S0955-2219(02)00139-5

CO_2–Ar gases) were introduced in the furnace. Oxygen partial pressure was controlled by changing the gas mixing ratios. CO_2 gas dissociates into CO and O_2 at high temperatures. The oxygen partial pressure (P_{O_2}) in CO_2 containing atmosphere was calculated from the thermodynamic data of CO_2–CO–O_2 system. The temperature of specimen was measured with a thermocouple (type-B) placed below the specimen within several millimeters.

The structure of the surface oxide layer was investigated by an X-ray diffractometer (XRD). The surface and cross-section of the specimen after the oxidation were observed by a scanning electron microscope (SEM) and an optical microscope.

3. Results and discussion

3.1. Active oxidation

Fig. 1 shows the relationship between mass change and oxygen partial pressure (P_{O_2}) at 1873 K in O_2–Ar, where P_{O_2} was increased with time. The mass loss became significant with increasing P_{O_2}. This mass loss behavior is termed as active oxidation. The active oxidation rates in O_2–Ar (k_a) were independent of time. The values of k_a increased linearly with P_{O_2}, and were proportional to nearly $V^{1/2}$ (V; gas velocity).[8] These suggest that the inward diffusion of oxidant in a gas boundary layer may be rate-controlling for the active oxidation. An abrupt change from the mass loss (active oxidation) to a small mass gain (passive oxidation) appeared at $P_{O_2} = 160$ Pa, which is called as active-passive transition oxygen partial pressure ($P_{O_2}{}^t$).

Wagner[9] proposed a model to explains the transition behavior for Si. By applying this model, the theoretical $P_{O_2}{}^t$ value may be given as Eq. (1).

$$P^t_{O_2} = 1/2\left(D_{SiO}/D_{O_2}\right)^{1/2} P^{eq}_{SiO} \quad (1)$$

where P^{eq}_{SiO} is the equilibrium vapor pressure of SiO(g), D_x is a diffusion constant of x-species in the gas boundary layer. The D_{SiO}/D_{O_2} ratio could be assumed as 0.8.[10] There are several probable thermal equilibria to calculate the P^{eq}_{SiO}. The most likely equation may be Eq. (2), because no C(s) or Si(s) phase was identified after the active oxidation.

$$SiC(s) + 2\ SiO_2(s) = 3\ SiO(g) + CO(g) \quad (2)$$

Fig. 2 summarizes the reported $P_{O_2}{}^t$ for single crystal, sintered and CVD SiC in O_2–Ar atmospheres.[10–14] The temperature dependence of experimental $P_{O_2}{}^t$ was in agreement with the calculated values from the Wagner model. The Wagner model could be fundamentally suitable to explain the transition behavior; however the experimental values were 1/10 to 1/100 times smaller than the calculated values. This model contains too simplified assumptions, and the constants used in the calculation may not be exactly precise at high temperatures. The modification of the Wagner model would be necessary to explain the transition behavior more accurately.

The active oxidation behavior of CVD SiC in CO–CO_2 atmosphere is depicted Fig. 3. The active oxidation rate in CO–CO_2 (K_{CO}) showed maxima at $P_{CO_2}/P_{CO} = 10^{-2}$ to 10^{-3}.[15] In the P_{CO_2}/P_{CO} region lower than the maxima, free carbon layer was found on the SiC surface. In the P_{CO_2}/P_{CO} region higher than the maxima, granular or porous layer of SiO_2 was observed on the SiC surface. The K_{CO} values in the P_{CO_2}/P_{CO} region higher than the maxima decreased with increasing P_{CO_2}/P_{CO}. This behavior is a contrast to that in O_2–Ar atmosphere. Fig. 4 represents the time dependence of

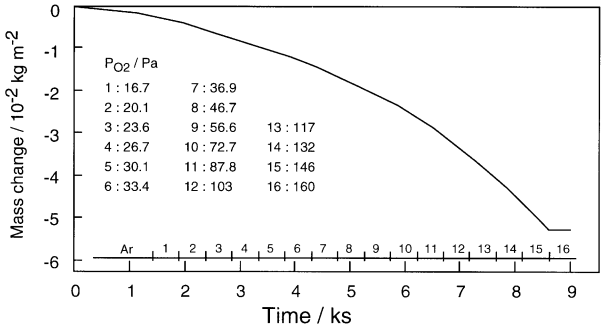

Fig. 1. Relationship between mass change of CVD SiC and oxygen partial pressure (P_{O_2}) at 1873 K.

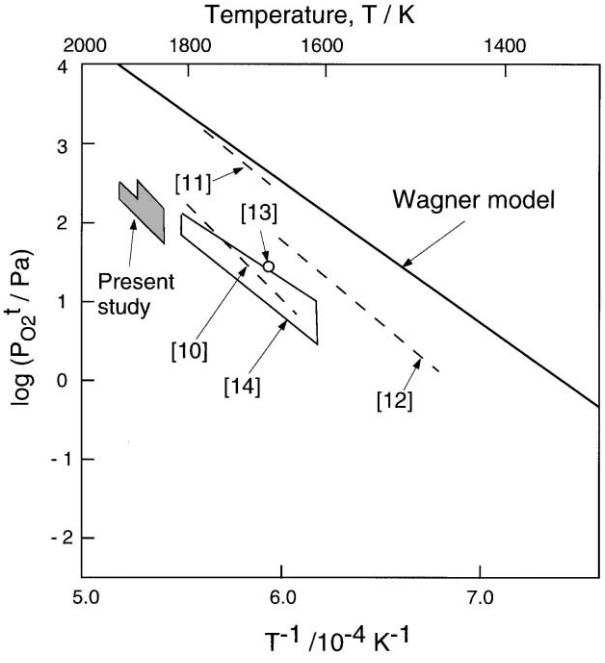

Fig. 2. Effect of temperature on active–passive transition oxygen partial pressure ($P_{O_2}{}^t$) for sintered, single crystal and CVD SiC.

mass change in CO–CO_2 at P_{CO_2}/P_{CO} = 1–9.[16] The mass loss decreased linearly with time. The k_{CO} values decreased with increasing P_{CO_2}/P_{CO}, and there was almost no mass change at P_{CO_2}/P_{CO} = 4, where the vaporization and formation of SiO_2 might have proceeded at almost the same rates. If the active-passive transition is defined as the condition for "a small mass gain", the transition P_{CO_2}/P_{CO} value would be 4 at 1873 K. On the other hand, if it is defined as the condition for "SiO_2 formation", the transition P_{CO_2}/P_{CO} would be 10^{-2} to 10^{-1}.

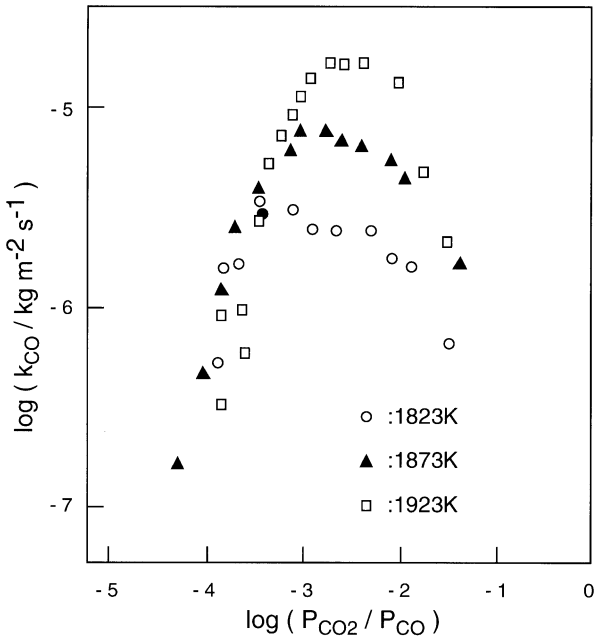

Fig. 3. Effect of P_{CO_2}/P_{CO} on active oxidation rates for CVD SiC in CO–CO_2.

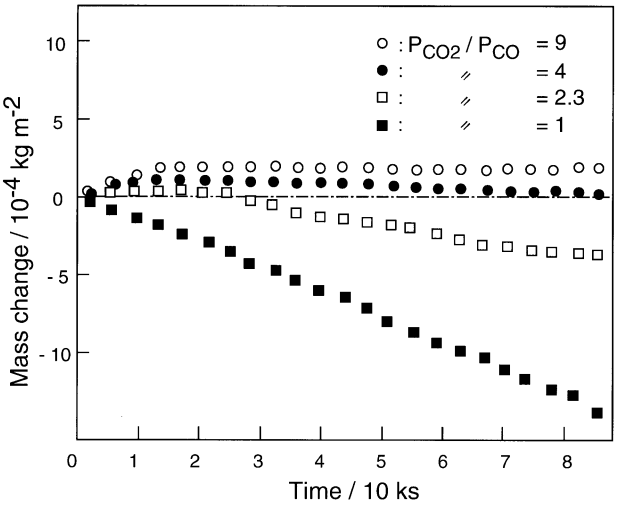

Fig. 4. Time dependence of mass change for CVD SiC at P_{CO_2}/P_{CO} = 1–9 and 1823 K in CO–CO_2.

Heuer et al.[17] have explained the active–passive transition of SiC and Si_3N_4 by using so-called volatility diagram. Fig. 5 demonstrates the calculated volatility diagram for Si–C–O system at 1873 K, in which the equilibrium vapor pressures of SiO(g) or SiO_2(g) and the stable solid phases are indicated as a function of P_{O_2} and P_{CO_2}/P_{CO} ratio. The transition should occur at P_{O_2} more than "isomolar line, Im" (the line of $P_{SiO} = 2P_{O_2}$) in O_2–Ar. Since the O_2 gas comes from the ambient atmosphere, the P_{SiO} should be less than $2P_{O_2}$. Only the higher P_{O_2} region than the Im line is physically meaningful, then eventually the $P_{O_2}{}^t$ should be somewhere more than the Im line. The experimental $P_{O_2}{}^t$ value (E_O) was obviously situated at more than the Im line and the calculated value from the Wagner model (W_O). On the other hand, in CO–CO_2, the transition P_{O_2} should be more than "Isobaric (Ib) line" (the line of $P_{SiO} = P_{CO}$). The calculated P_{CO_2}/P_{CO} from the Wagner model (W_{CO}) and experimental value (E_{CO}) are indicated in Fig. 5. At $P_{CO_2}/P_{CO} = 10^{-2}$ to 10^{-1} the decomposition and formation of SiO_2 would have proceeded simultaneously. The E_{CO} would mean the condition where the decomposition and the formation of SiO_2 occur at the same rate. The Wagner model does not take into account the decomposition of SiO_2. The model simply predicts the lowest P_{CO_2}/P_{CO} condition for the SiO_2 formation. The experimental P_{CO_2}/P_{CO} for the SiO_2 formation was almost in agreement with the W_{CO} value.

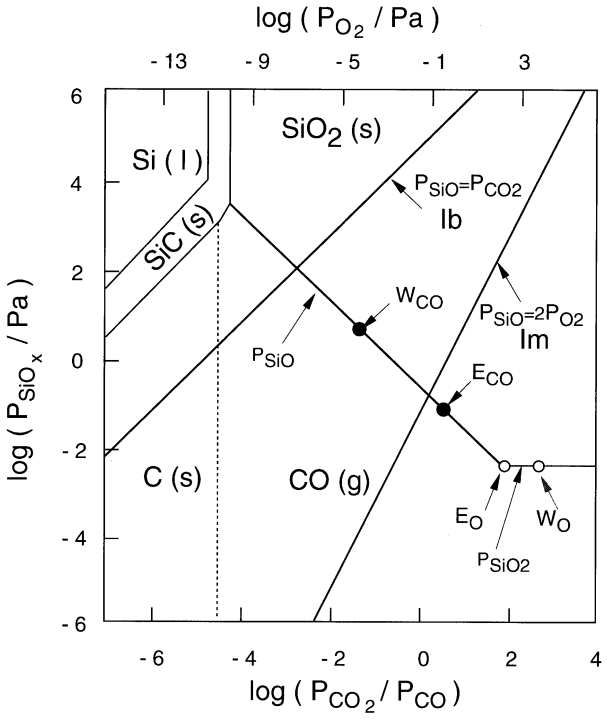

Fig. 5. Volatility diagram for the Si–C–O system at 1873 K. E_O: experimental $P_{O_2}{}^t$ in O_2–Ar, W_O: calculated $P_{O_2}{}^t$ in O_2–Ar. E_{CO}: experimental $P_{O_2}{}^t$ in CO–CO_2, W_{CO}: calculated $P_{O_2}{}^t$ in CO–CO_2.

3.2. Passive oxidation

There are many reports published on the oxidation rate (k_p; parabolic rate constant) for SiC. Fig. 6 summarizes the effect of mainly impurities on the k_p values.[18] Numbers given in the parentheses represent the impurity content in mass%. Sintering aid such as B and C might not cause degradation of oxidation resistance; however, an additive like Al_2O_3 would react with SiO_2 to form silicate phase. Since the diffusion rates of oxidants or oxidation products in the silicate phase is higher than those in pure silica, the oxidation resistance of SiC sintered bodies containing oxide additives were significantly degraded.

Opila and Nguyen[3] have studied the oxidation of CVD SiC in CO_2 at temperatures from 1473 to 1673 K by thermogravimetry; however they have not detect significant mass change. Fitzer and Ebi[4] reported the parabolic mass gain in CO_2 at 1673 K, but at 1773 K the behavior was too complicated (i.e. parabolic mass gain initially, and sharp mass loss in later periods). Antill and Warburton[5] reported that the oxidation rates in CO_2 were 1/20 times slower than those in O_2 at temperatures from 1273 to 1573 K; however the mass change curves were not presented.

We have measured the passive oxidation behavior of high purity CVD SiC in O_2 and CO_2. Fig. 7 shows the relationship between time and mass gain in pure O_2 in both logarithmic scale. The gradient of the line was half at 1773 K indicating parabolic kinetics. At 1910 K, on the other hand, the gradient was one in the initial stage up to 60 ks indicating linear kinetics, then the gradient changed to half indicating parabolic kinetics. This behavior is commonly called as "linear–parabolic" kinetics. In O_2, the oxidation kinetics was either parabolic or linear–parabolic depending on temperature and P_{O_2}, whereas it was always parabolic in CO_2. Fig. 8 summarizes the behavior of oxidation kinetics as functions of temperature and P_{O_2}. The boundary between linear-parabolic and parabolic kinetics was independent of gas species, but depended on P_{O_2} and temperature.

Fig. 9 represents the Arrhenius plot of linear oxidation rates (k_l) obtained in the linear-parabolic region. The activation energy was independent of P_{O_2}, being 110 kJ/mol. Ramberg et al.[19] found the linear–parabolic behavior for single crystal and CVD SiC in O_2, and reported that the activation energy of k_l was 94–164 kJ/mol. This value is close to the value of present work, suggesting a similar rate-controlling step. They have not explained the mechanism of linear oxidation.

Fig. 10 represents the P_{O_2} dependence of k_p at 1900 K in O_2–Ar and CO_2–Ar. In both atmospheres, the relationship between k_p and P_{O_2} was represented as $k_p \propto P_{O_2}{}^n$, where $n = 0.08$–0.18 in O_2–Ar, and $n = 0.37$ to 0.53 in CO_2–Ar at temperatures from 1875 and 1985 K. The weak P_{O_2} dependence in O_2–Ar suggests that the parabolic oxidation may be controlled by the outward diffusion of oxide vacancy or CO molecule. The strong P_{O_2} dependence in CO_2–Ar, on the other hand, may be caused of inward diffusion of oxidant. Since the molecule size of CO_2 (0.3 nm in dia.) is bigger than oxide ion, O^{2-} (0.14 nm in dia.), the diffusion of interstitial O^{2-} may be rate-controlling in CO_2–Ar.

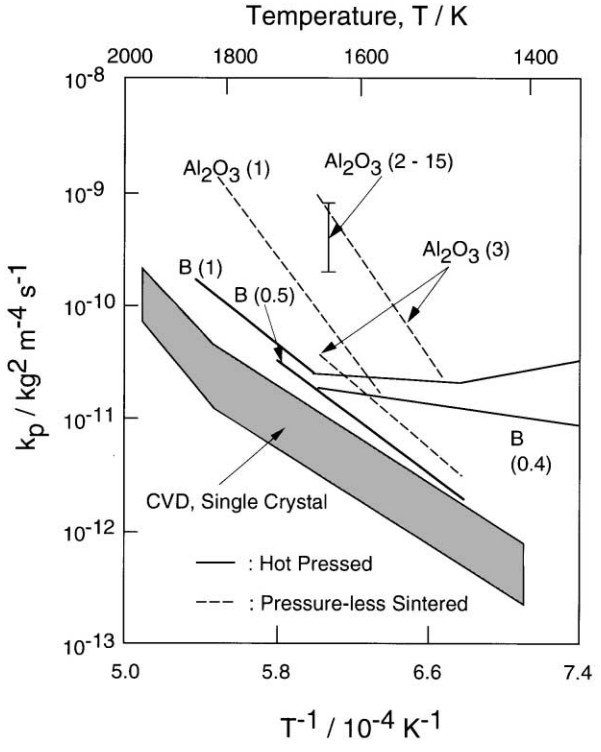

Fig. 6. Effect of temperature on parabolic rate constant for sintered, single crystal and CVD SiC. Additives and their contents (mass%) are indicated for sintered SiC.

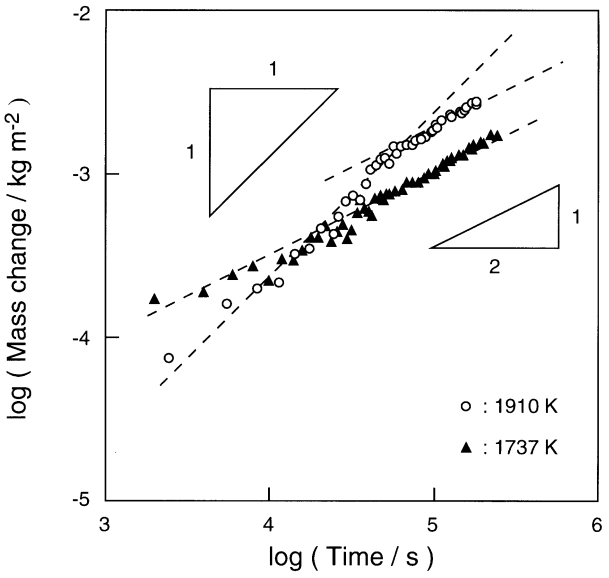

Fig. 7. Time dependence of mass change in O_2 ($P_{O_2} = 0.1$MPa) at 1737 and 1910 K for CVD SiC in logarithmic scales.

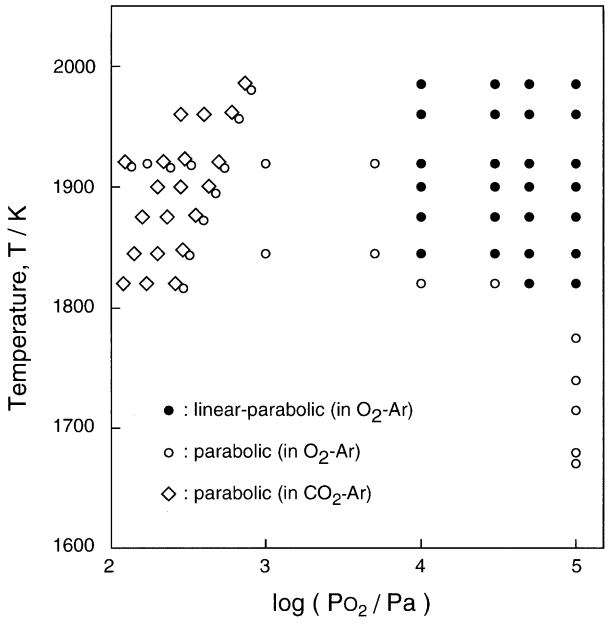

Fig. 8. Effects of temperature and P_{O_2} on the oxidation behavior for CVD SiC in O_2–Ar and CO_2–Ar.

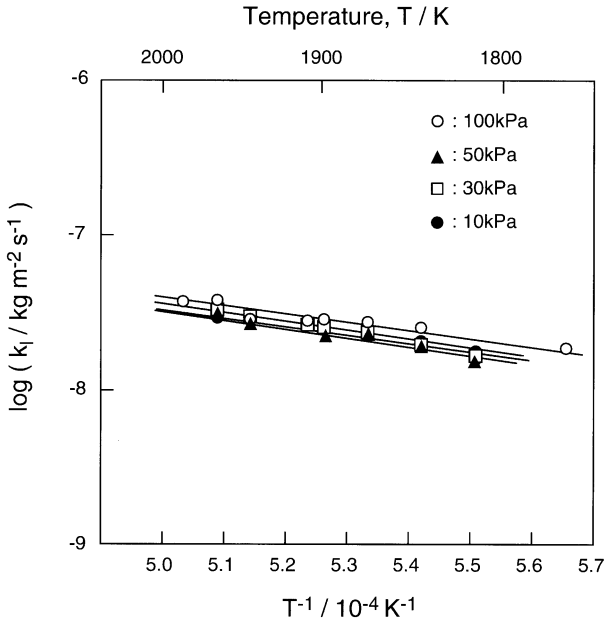

Fig. 9. Temperature dependence of linear oxidation rates (k_l) for CVD SiC in O_2 (P_{O_2} = 0.1 MPa).

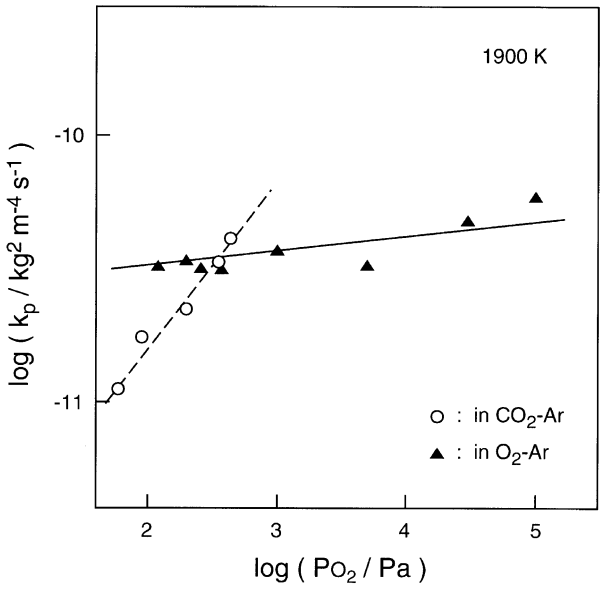

Fig. 10. Effect of P_{O_2} on parabolic rate constant (k_p) for CVD SiC in O_2–Ar and CO_2–Ar.

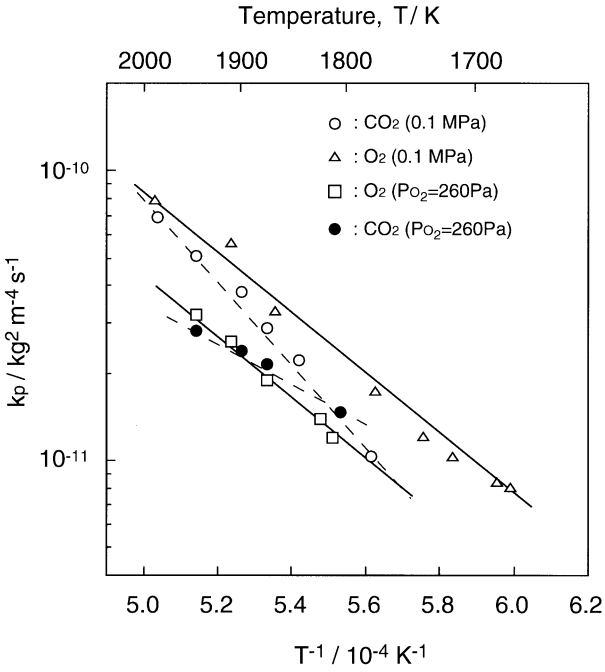

Fig. 11. Effect of temperature on the parabolic rate constants (k_p) in O_2–Ar and CO_2–Ar.

Fig. 11 represents the Arrhenius plot of k_p obtained in pure CO_2 and pure O_2. The activation energy in pure CO_2 (290 kJ/mol) was greater than that in pure O_2 (210 kJ/mol). However, if the oxidant in CO_2 is not CO_2 molecule but dissociate oxygen, the k_p values should be compared under the same P_{O_2}. The k_p values at P_{O_2} = 260 Pa in O_2–Ar and CO_2–Ar are also plotted in Fig. 11. The activation energy at P_{O_2} = 260 Pa in O_2–Ar is 210 kJ/mol, which is in agreement with that in pure O_2. On the other hand, the activation energy at P_{O_2} = 260Pa in CO_2–Ar is 150 kJ/mol, which is much smaller than that in pure CO_2. The difference of activation energy between O_2 (210 kJ/mol) and CO_2 (150 kJ/mol) also suggests the different rate-controlling step between these atmospheres. Fig. 12 summarizes the K_p values for single crystal and CVD SiC in O_2.[20–24] The activation energy values have ranged from 120 to 400 kJ/mol in the literature. There is a general trend that the higher temperature the greater the activation energy. It is commonly accepted that the relatively low activation energy of

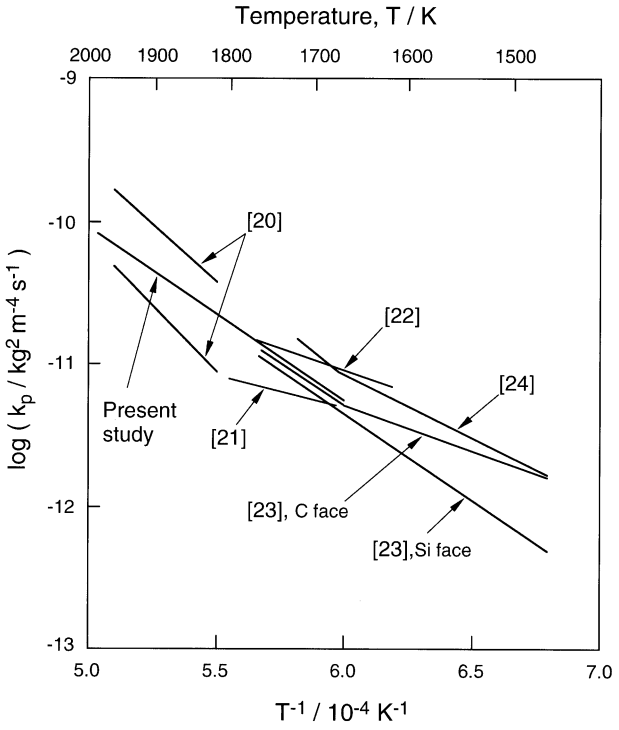

Fig. 12. Comparison of parabolic rate constants (k_p) for single crystalline and CVD SiC in literatures with those of present study.

80–120 kJ/mol may correspond to the permeation of oxygen molecule in amorphous silica, and the high activation energy of 230–400 kJ/mol may suggest the diffusion of oxide ion in amorphous silica or cristobarite.[2] The activation energy value obtained in the present work (210 kJ/mol in O_2) is close to value for the vacancy diffusion of oxide ion.

3.3. Bubble formation

A few papers have reported the bubble formation at less than 1773 K in hot-pressed (HP) SiC.[6,7] Since HP SiC bodies are added with metal oxides such as Al_2O_3, silicate phases are contained in the oxide layer. The melting point of pure silica is generally higher than that of silicates, thus the bubble formation temperature of CVD SiC must be higher than that of impure SiC sintered bodies. Schiroky[6] and Jacobson[1] reported the bubble formation at 1973–2023 K and at 2073 K for CVD SiC, respectively. However, no paper reported the effect of gas species or P_{O_2} on the bubble formation of CVD SiC.

Fig. 13 depicts the cross-section of bubbles formed at 1990 K in O_2–Ar ($P_{O_2}=100$ kPa). The thermogravimetry is advantageous to detect the bubble formation because mass change curves indicate characteristic zigzag-shapes due to the sequence of bubble-formation and -rupture. Fig. 14 shows the time dependence of mass change at 1985 K and $P_{O_2}=10$ kPa, which is a transition condition from linear–parabolic to bubble

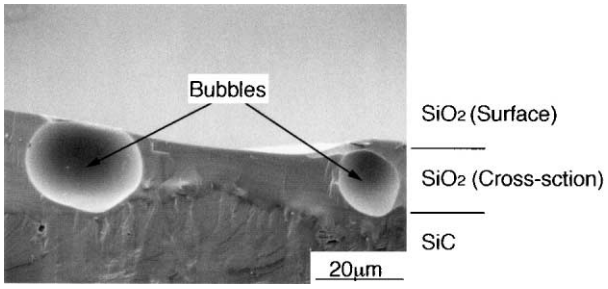

Fig. 13. Cross-section of silica layer with bubbles formed at 1990 K in O_2–Ar ($P_{O_2}=100$ kPa).

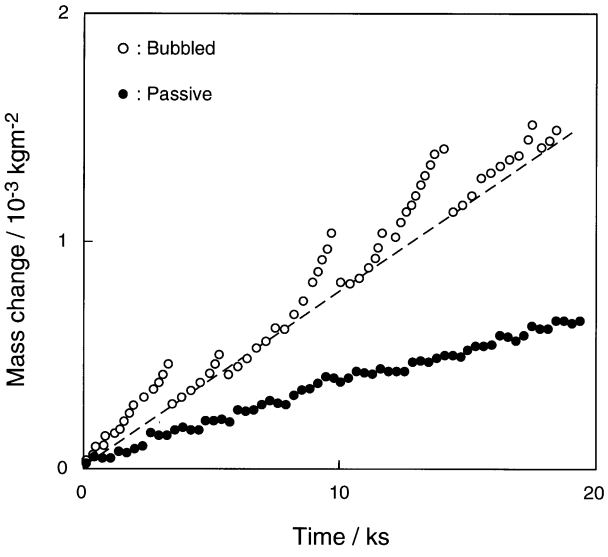

Fig. 14. Time dependence of mass change at 1985 K and $P_{O_2}=10$ kPa.

formation. When the bubble formed, the linear oxidation rates were accelerated and the zigzag-shaped mass gain was overlapped with the linear mass gain. Fig. 15 demonstrates a transition condition from parabolic to bubble formation (i.e. 1965 K and $P_{O_2}=700$ Pa), where the significant zig-zag mass change curve was overlapped with the parabolic mass gain. Fig. 16 depicts the effects of temperature and P_{O_2} on the boundary between passive and bubble formation. The boundary changed depending on temperature and P_{O_2}, but being independent of the gas species (i.e. O_2 or CO_2). At $P_{O_2} > 5$ kPa, the transition from linear-parabolic to bubble formation took place at around 1985 K. At $P_{O_2} < 5$ kPa, the transition temperature was broader and decreased with decreasing P_{O_2}. The bubbles should form when the total pressure (P_{tot}) inside the bubbles exceeds at least the ambient gas pressure (0.1 MPa). Since CO gas accumulates at the SiC/SiO_2 interface, the carbon activity (a_c) may increase and finally reach to unity.[25] Fig. 17 demonstrates the temperature dependence of P_{tot} in the bubble for the following two cases. The one is that carbon-saturated SiC ($a_c=1$) reacts with SiO_2, and the other is that the stoichiometric reaction of Eq. (3) proceeds at the SiC/SiO_2 interface.

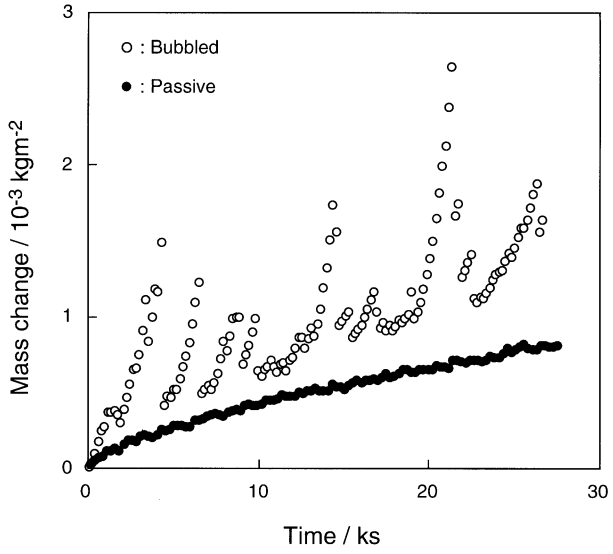

Fig. 15. Time dependence of mass change at 1965 K and $P_{O_2} = 700$ Pa.

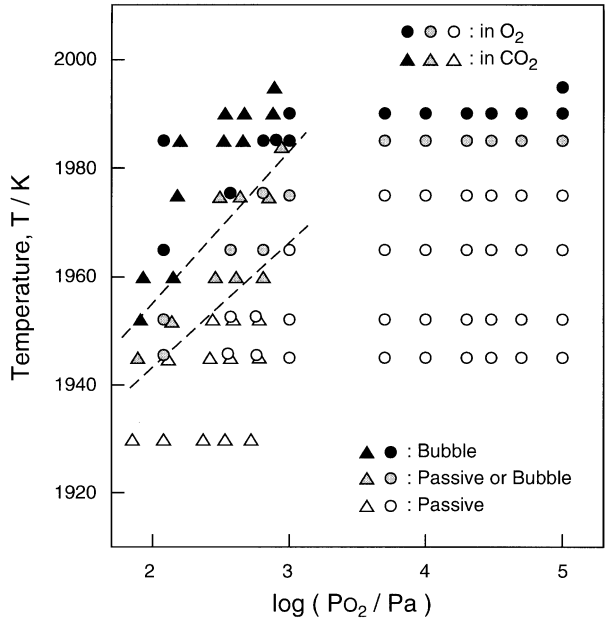

Fig. 16. Effects of temperature and P_{O_2} on the boundary between passive oxidation and bubble formation in O_2–Ar and CO_2–Ar atmospheres.

$$SiC(s) + 2SiO_2(s) = 3SiO(g) + CO(g) \quad (3)$$

The transition temperature at $P_{O_2} > 5$ kPa was about 1985K. This may suggest the slight increase of a_c at the SiC/SiO_2 interface. At $P_{O_2} < 5$ kPa, the transition temperature decreased with decreasing P_{O_2}. The CO:CO_2 ratio calculated from the CO_2–CO–O_2 equilibrium should increase with decreasing P_{O_2} in CO_2–Ar. The increase of CO partial pressure in the ambient atmosphere might increase the a_c significantly at the SiC/SiO_2 interface. This might have decreased the bubble formation temperature.

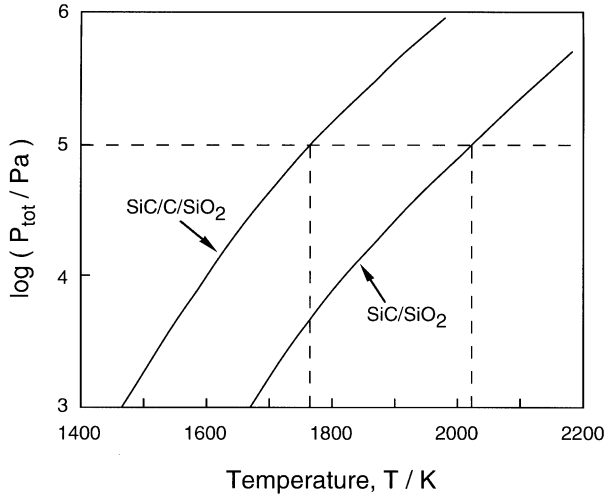

Fig. 17. Temperature dependence of total pressure inside bubbles (P_{tot}) for the carbon saturated and the stoichiometric conditions.

4. Summary

The transition from active to passive oxidation in O_2–Ar was clearly observed. The active oxidation rates in O_2–Ar increased with increasing P_{O_2}. The active oxidation rates in CO–CO_2 (K_{CO}) showed the maxima at about $P_{CO_2}/P_{CO} = 10^{-2}$. The K_{CO} values decreased with increasing P_{CO_2}/P_{CO}, and the active oxidation gradually changed to the passive oxidation. The active–passive transition in both atmospheres could be explained by the Wagner model and the volatility diagram.

The passive oxidation was classified into linear–parabolic and parabolic behavior depending on temperature and P_{O_2}. In O_2–Ar, the parabolic rate constant (k_p) values were almost independent of P_{O_2}, and the activation energy for the parabolic oxidation was 210 kJ/mol. In CO_2–Ar, the k_p values increased significantly with increasing P_{O_2}, and the activation energy was 150 kJ/mol. The oxidation kinetics could be different between these atmospheres.

In much higher temperature region, the bubble formation was observed in O_2–Ar and CO_2–Ar. The transition from passive oxidation to bubble formation depended on P_{O_2} and temperature. The linear and parabolic oxidation rates were accelerated by the bubble formation.

References

1. Jacobson, N. S., Corrosion of silicon-based ceramics in combustion environments. *J. Am. Ceram. Soc.*, 1993, **76**, 3.
2. Narushima, T., Goto, T., Hirai, T. and Iguchi, Y., High-temperature oxidation of silicon carbide and silicon nitride. *Mater. Trans. JIM*, 1997, **38**, 821.
3. Opila, E. J. and Nguyen, Q. N., Oxidation of chemically-vapor-deposited silicon carbide in carbon dioxide. *J. Am. Ceram. Soc.*, 1998, **81**, 1949.

4. Fitzer, E. and Ebi, R., Kinetics studies on the oxidation of silicon carbide. In *Silicon Carbide 1973*, ed. R. C. Marshall, J. W. Faust Jr. and C. E. Ryan. University of South Carolina Press, USA, 1974, pp. 320.
5. Antill, J. E. and Warburton, J. B., Oxidation of silicon and silicon carbide in gaseous atmospheres at 1000–1300 °C. In *Reactions between Solids and Gases* (AGARD CP-52), 1970, 10.
6. Schiroky, G. H., Mitchell, T. E. and Heuer, A. H., Oxidation behavior of chemically vapor-deposited silicon carbide. *Adv. Ceram. Mater*., 1987, **2**, 137.
7. Mieskowski, D. M., Mitchell, T. E. and Heuer, A. H., Bubble formation in oxide scale on SiC. *Comm. Am. Ceram. Soc., c-, 1984, 17*.
8. Narushima, T., Goto, T., Iguchi, Y. and Hirai, T., High-temperature active oxidation of chemically vapor-deposited silicon carbide in an Ar–O_2 atmospheres. *J. Am. Ceram. Soc*., 1991, **74**, 2583.
9. Wagner, C., Passivity during the oxidation of silicon at elevated temperatures. *J. Appl. Phys*, 1958, **29**, 1259.
10. Hinze, J. W. and Graham, H. C., The active oxidation of Si and SiC in the viscous gas-flow regime. *J. Electrochem. Soc*., 1976, **123**, 1066.
11. Balat, M., Flamant, G., Male, G. and Pichelin, G., Active to passive transition in the oxidation of silicon carbide at high temperature and low pressure in molecular and atomic oxygen. *J. Mater. Sci*., 1992, **27**, 697.
12. Gulbransen, E. A., Andrew, K. F. and Brassart, F. A., The oxidation of silicon carbide at 1150 ° to 1400 °C and at 9×10^{-3} to 5×10^{-1} torr oxygen pressure. *J. Electrochem. Soc*., 1966, **113**, 1311.
13. Kim, H. E. and Moorhead, A. J., Effects of active oxidation on the flexural strength of α-Silicon Carbide. *J. Am. Ceram. Soc*., 1990, **73**, 1868.
14. Vaughn, W. L. and Maahs, H. G., Active-to-passive transition in the oxidation of silicon carbide and silicon nitride in air. *J. Am. Ceram. Soc*., 1990, **73**, 1540.
15. Narushima, T., Goto, T., Yokoyama, Y., Iguchi, Y. and Hirai, T., High-temperature active oxidation of chemically vapor-deposited silicon carbide in CO–CO_2 atmosphere. *J. Am. Ceram. Soc*., 1993, **76**, 2521.
16. Narushima, T., Goto, T., Yokoyama, Y., Takeuchi, M., Iguchi, Y. and Hirai, T., Active-to-passive transition and bubble formation for high-temperature oxidation of chemically vapor-deposited silicon carbide in CO–CO_2 atmosphere. *J. Am. Ceram. Soc*., 1994, **77**, 1079.
17. Heuer, A. and Lou, V. L. K., Volatility diagrams for silica, silicon nitride and silicon carbide and their application to high-temperature decomposition and oxidation. *J. Am. Ceram. Soc*., 1990, **73**, 2785.
18. Goto, T., Oxidation resistance of silicon-based ceramics. *Corr. Eng*., 1999, **48**, 169.
19. Ramberg, C. E., Cruciani, G., Spear, K. E., Tressler, R. E. and Ramberg, C. F. Jr., Passive-oxidation kinetics of high-purity silicon carbide from 800° to 1100 °C. *J. Am. Ceram. Soc*., 1966, **79**, 2987.
20. Narushima, T., Goto, T. and Hirai, T., High-temperature passive oxidation of chemically vapor deposited silicon carbide. *J. Am. Ceram. Soc*., 1989, **72**, 1386.
21. Schiroky, G. H., Price, R. J. and Sheehan, J. E., Oxidation Characteristics of CVD Silicon Carbide and Silicon Nitride (Rept. No. GA-A18696). GA Technologies, 1986.
22. Ogbuji, L. U. J. T. and Opila, E. J., A comparison of the oxidation kinetics of SiC and Si_3N_4. *J. Electrochem. Soc*., 1995, **142**, 925.
23. Zheng, Z., Tressler, R. E. and Spear, K. E., Oxidation of single-crystal silicon carbide part I. experimental studies. *J. Electrochem. Soc*., 1990, **137**, 854.
24. Costello, J. A. and Tressler, R. E., Oxidation kinetics of silicon carbide crystals and ceramics: I, in dry oxygen. *J. Am. Ceram. Soc*., 1986, **69**, 674.
25. Jacobson, N. S., Lee, K. N. and Fox, D. S., Reaction of silicon carbide and silicon(IV) oxide at elevated temperatures. *J. Am. Ceram. Soc*., 1992, **75**, 1603.